(Received 26 September 2025, Accepted 27 March 2026, Scheduled 21 April 2026)

Design and Implementation of a High Gain Compact IoT Wearable Antenna for Vital Signs Data Transmission Using ESP8266

Rama K. Merugumalli[1, 2, *] and Subba R. Chalasani[3]

[1] Department of ECE, SRM Institute of Science and Technology, Kattankulathur 603203, Tamilnadu, India
[2] Department of ECE, Vasireddy Venkatadri International Technological University, Andhra Pradesh 522508, India
[3] Department of ECE, PVP Siddhartha Institute of Technology, Vijayawada 520007, Andhra Pradesh, India

ABSTRACT: This study presents a compact patch antenna in the form of a circle, suitable for use in medical and wearable Internet of Things (IoT) devices. The recommended antenna has been proposed to operate on a polyamide material with a dielectric constant of 3.5 and loss tangent of 0.008, at 2.4 GHz and 5.8 GHz bands. The IoT wearable antenna has a specific absorption rate (SAR) obtained at 2.4 GHz that is 0.6 W/kg, while at 5.8 GHz, it is 0.8 W/kg for 1 g of body tissue. Both values are significantly below the FCC exposure limit, confirming the safe operation of the compact IoT-enabled wearable antenna. The antenna achieves simulated gains of 7.54 dBi and 7.96 dBi with radiation efficiencies of 85.45% and 87.55% at 2.4 GHz and 5.8 GHz, respectively. The proposed system integrates the proposed antenna with an ESP8266 microcontroller, which enables the transmission of vital signs data over an IoT platform. A Modbus protocol and Node-RED platform are utilized for data acquisition, processing, and visualization. This makes it a small, cheap, and reliable solution for IoT-enabled healthcare systems.

1. INTRODUCTION

The current economic situation has a significant impact on the elderly population in the healthcare sector. Hospitals are often unwilling to allocate funds for services that are specifically designed for senior citizens [1]. The proposed dual-band wearable antenna enables data to be transmitted off the body quickly and reliably, as shown in Fig. 1, and is useful for remote health monitoring applications. It is important to acknowledge that the life expectancy of elderly individuals has increased as a result of technological advancements and medical diagnostics, and that technology has also contributed to their overall well-being. The IoT is advancing in a variety of fields [2], and wearable medical fields [3] have become a fundamental component of body area networks because of their ability to monitor vital signs in real time, including body temperature, oxygen saturation (SpO_2), and pulse rate.

An energy-efficient [4] health-monitoring system is equipped with a dual-band antenna that reduces electromagnetic interference. The system includes a health status display, real-time alerts, Bluetooth low-energy (BLE)/Wi-Fi communication [5], and three adaptive measurement modes to reduce power consumption [6]. Owing to improvements in flexible electronics, "smart" wearable market is one of the fastest growing sectors of the IoT [7]. These are IoT devices that can be worn on the body or attached to the skin and are designed to track important information about a person or his/her surroundings in real time [8]. Wearable antennas

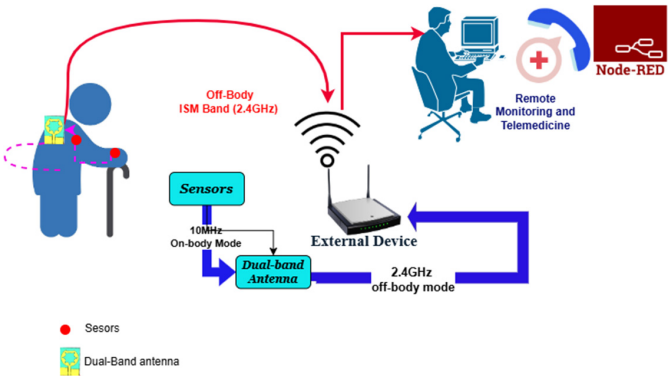

FIGURE 1. Block diagram of the dual-band wearable antenna for off-body data transmission in remote health monitoring.

produce a significant amount of electromagnetic radiation on the human body because of the proximity to the surface [9]. The health of humans will be compromised when the radiation is excessively high. The Federal Communications Commission (FCC) states that the SAR must meet its standards [10]. The maximum SAR value is 1.6 W/kg in the US (1 g standard) and 2.0 W/kg in Europe (10 g standard) [11].

Metamaterials are often used to mitigate the effects of SAR on the human body by lowering the antenna's back radiation and increasing its forward radiation [12]. Textile [13] or denim fabric [14] is often used to fabricate the substrates of wearable antennas for increased comfort. The conductive material can be either a conductive slurry [15] or conductive cloth [16]. The

* Corresponding author: Rama Krishna Merugumalli (rm0555@srmist.edu.in).

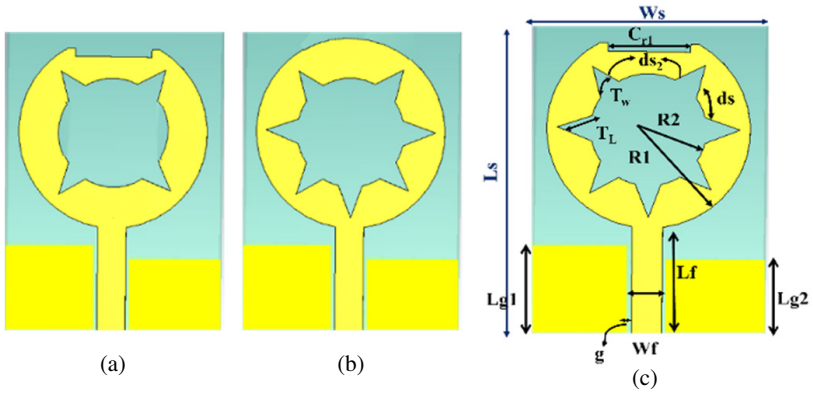

FIGURE 2. Stepwise iterations of antenna. (a) Iteration 1. (b) Iteration 2. (c) Proposed antenna.

antenna structure can be more compact [17], and its size can be reduced by utilizing a coplanar waveguide input [18]. A flexible substrate based on a polymer is employed to construct a triangular patch antenna [19]. The SAR of a monopole antenna is evaluated both with and without an artificial magnetic conductor (AMC) plane. The maximal SAR value decreased by 89.45% with respect to the antenna without an AMC, as indicated by the evaluation results [20]. A 2.4 GHz wireless sensor node has been optimized for use on the body in wearable applications [21]. The creation of an IoT cloud platform based on Message Queuing Telemetry Transport (MQTT), with a flow design by Node-RED, helps developers set up the IoT platform on their own to send data, process data, and show it on the dashboard [22].

2. DESIGN METHODOLOGY OF ANTENNA

The antenna's fundamental design is a circular patch that utilizes a coplanar waveguide (CPW) feeding technique, as shown in Fig. 2. Polyamide is a passive dielectric substrate that does not consume electrical energy. Only dielectric loss contributes to radio frequency (RF) absorption. The flexible polyimide substrate was used for antenna design with a loss tangent of 0.008 and a dielectric constant of 3.5, which results in very minimal EM absorption. Consequently, the power loss in the substrate was minimal, and the antenna maintained high radiation efficiency, indicating negligible energy dissipation in the material. Furthermore, polyamide exhibits very low moisture absorption ($< 0.5\%$), which minimizes variations in dielectric properties and prevents detuning under sweaty and humid environmental conditions. The material also demonstrates excellent thermal stability with an operational endurance ranging from $-60°$C to $250°$C, ensuring dimensional stability and consistent antenna performance under body temperature, outdoor heating, and long-term wearable usage. Therefore, the proposed antenna remains mechanically robust and electromagnetically reliable even under moisture and thermal exposure conditions.

TABLE 1. The proposed antenna dimensions.

Parameter	Units (mm)	Parameter	Units (mm)
Ls	40	Wf	2.85
Ws	28	Lf	9.62
h	0.1	$Lg1$	11.68
$R1$	12.6	$Lg2$	10
$R2$	7.15	$ds1$	2.58
g	0.15		

The antenna dimensions were $40 \times 28 \times 0.1\,\text{mm}^3$. The circular patch had the outer and inner circle radii of 12.6 mm and 7.15 mm, respectively. Subsequently, the circular patch was equipped with star-shaped arms. The antenna received power from a 50-ohm strip line with CPW feeding. The compact IoT-enabled wearable antenna's dimensions are shown in Table 1.

This formula is typically used to determine the radius $R1$ of the patch, which indicates the structure of the circular ring.

$$R1 = \frac{F}{\left\{1 + \frac{2h}{\pi\varepsilon_r}\left[\ln\left(\frac{\pi F}{2h}\right) + 1.7726\right]\right\}^{1/2}} \tag{1}$$

$$F = \frac{8.791 \times 10^9}{f_r\sqrt{\varepsilon_r}} \tag{2}$$

where h is the substrate height, and ε_r is the dielectric constant. The patch with inner ring radius $R2$ and six-star points (arms) can be obtained as

$$R2 = \frac{d_s}{2\sin\left(\frac{\pi}{N}\right)} \tag{3}$$

where $d_s = 2.58$ mm is the distance between star-shaped arms.

3. RESULTS AND DISCUSSIONS

Figure 3(a) shows the antenna design process, which underwent multiple evaluations to achieve the best performance in transmitting vital signs across the IoT. In iterations 1, 2, and 3, this antenna did not resonate in the Industrial, Scientific, and Medical (ISM) band. In iteration 4, the antenna resonated effectively at 2.4 GHz and 5.8 GHz, covering both ISM bands. Fig. 3(b) illustrates the gain and efficiency performance evaluation of the proposed antenna. At 2.4 GHz, the antenna has a gain of 7.545 dBi and 85.45% efficiency, and at 5.8 GHz, there is 7.96 dBi gain and 87.55% efficiency.

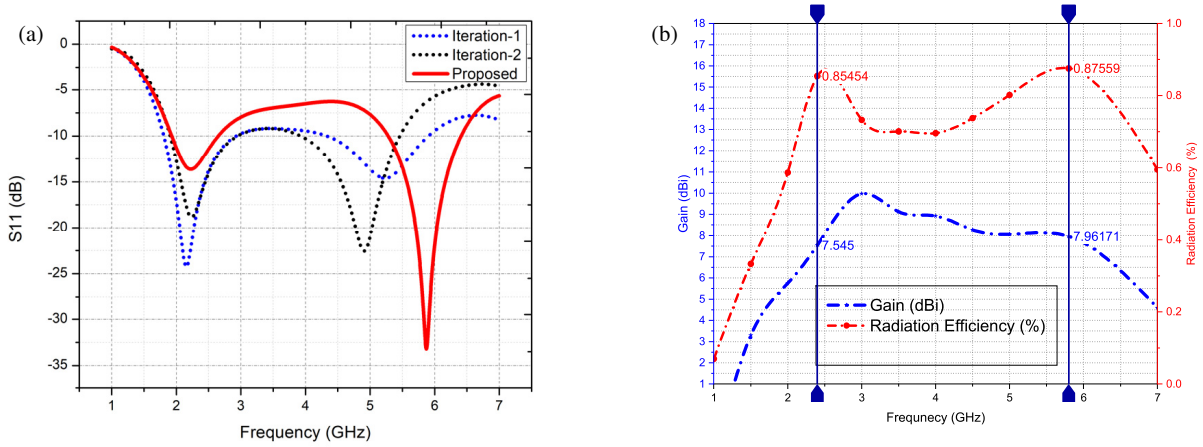

FIGURE 3. (a) S_{11} evaluation for antenna iterations, (b) simulated gain and efficiency of the proposed antenna.

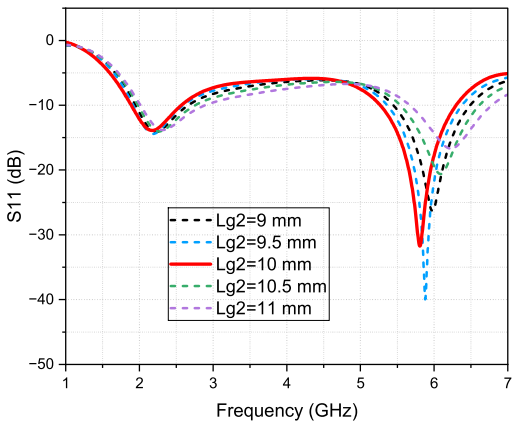

FIGURE 4. S_{11} characteristics with $Lg2$ variations.

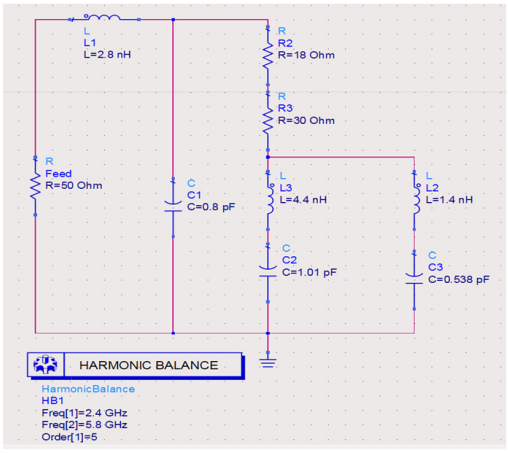

FIGURE 5. Equivalent circuit of the proposed antenna.

A parametric study of the ground length ($Lg2$) was done to justify the choice of the CPW ground dimensions. The dependence of S_{11} on the length of the ground is shown in Fig. 4. As can be observed, the ground length has a large influence on the resonant properties of the antenna. The $Lg2$ value of 10 mm gives stable two-band resonances at 2.4 GHz and 5.8 GHz with better impedance matching. Thus, this value was chosen in the final design of the antenna.

The results show that both ISM bands have good radiation efficiency and steady gain. These frequency bands are ideal for short-range, low-power communication, which makes the antenna suitable for wearable biomedical IoT devices that need to reliably monitor vital parameters, such as heart rate and SpO_2 transmission using ESP8266-based systems.

The 2.4 GHz and 5.8 GHz resonances are modeled as the equivalent circuit of the proposed antenna, as shown in Fig. 5. The network of L-type (L3 and C3) is matched with a feed impedance 50-Ohm, and two parallel RLC networks (R1, L1, C1) and (R2, L2, C2) are the antenna resonant modes.

$$\omega_o = \frac{1}{\sqrt{LC}} \tag{4}$$

where $\omega_o = 2\pi f$ is the angular frequency, branch impedance at the required resonance given as

$$Z_{RLC} = R + j\omega L + \frac{1}{j\omega C} \tag{5}$$

The reactive components cancel at resonance and only result in resistive impedance. Appropriate values of L and C enable the circuit to have good matching ($S_{11} < -10$ dB) at both bands.

3.1. Performance Analysis of the Compact IoT-Enabled Wearable Antenna under Simulation and Measurement

The fabricated IoT wearable antenna is shown in Fig. 6(a). It has a small and low-weight design, which is appropriate in wearable applications. Fig. 6(b) illustrates the Vector Network Analyzer (VNA) measurement configuration, and the obtained S_{11} values are very similar to the simulated response of the dual-band response in Fig. 6(c).

Measurement of the radiation pattern and gain of the antenna was conducted in a fully anechoic chamber, as shown in Fig. 7, in order to guarantee the far-field condition and minimize external interference. RF absorbers in the form of pyramids were

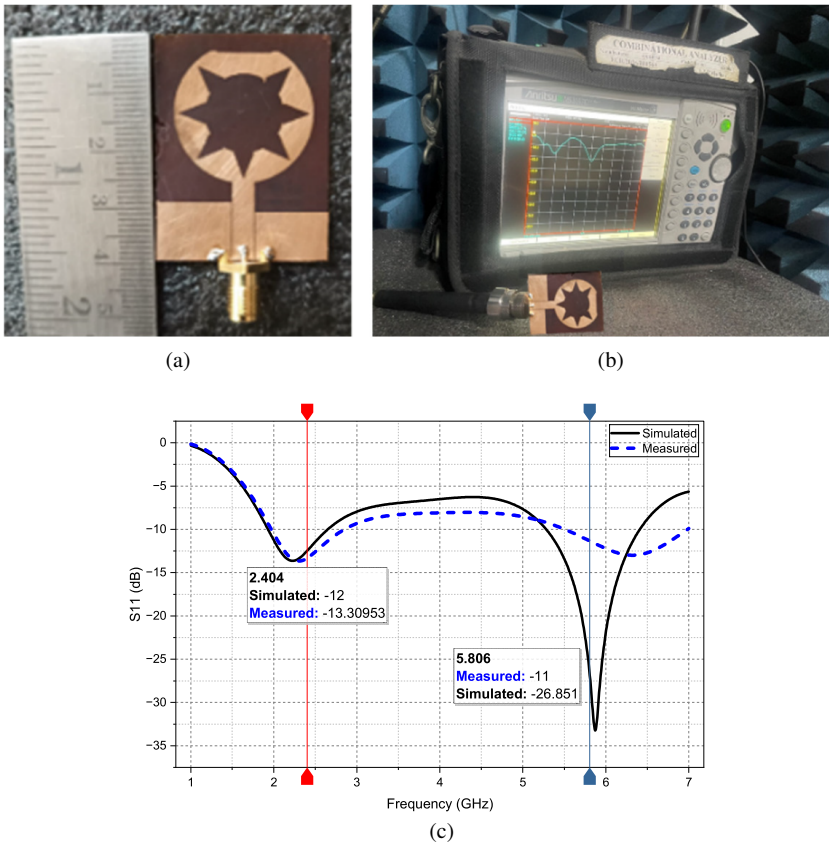

FIGURE 6. (a) Fabricated prototype. (b) Antenna measurement experimental setup. (c) Simulated vs. measured S_{11} characteristics.

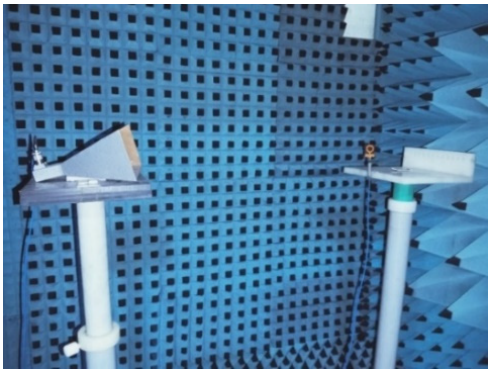

FIGURE 7. Far-field anechoic chamber measurement setup.

installed in the chamber, which gave the reflections of less than -40 dB at the frequency range in which it was operated. The far-field condition was met by the distance between the antenna under test (AUT) and the reference antenna.

The deviation between simulated and measured results is noticeable at higher frequencies due to the increased sensitivity of antenna characteristics to fabrication tolerances and slight variations in the substrate's electrical properties.

Figure 8 shows the peak gain of the compact IoT-enabled wearable antenna for the two operating frequencies. The gain at the first resonance for the simulation was 7.545 dBi; however, the gain was slightly lower at 6.45 dBi for the measurement. The gain at the second resonance for the simulation was 7.961 dBi, whereas the gain was 6.86 dBi for the measurement. The close match between the simulated and measured results demonstrates that the design process was accurate and that the proposed antenna will perform well in IoT-based vital signal transmission applications.

Measurement repeatability and uncertainty analysis were performed for both S_{11} and gain measurements to achieve the reliability of the experimental results. The tests were performed thrice, $N = 3$, under the same test conditions. The S_{11} findings showed a significant reproducibility with the largest standard deviation of 0.12 dB between repeated readings. Similarly, the measurements of the realized gain revealed a within-repetition variation of less than 0.45 dB. The total uncertainty of the measurement system was estimated using the VNA calibration tolerance, stability of the cable, error in the alignment of the antenna, and effects of the anechoic chamber environment. The obtained results prove that the reported performance values are experimentally reliable, repeatable, and stable.

3.2. Surface current Distribution

Figures 9(a) and 9(b) demonstrate the surface current distribution of the proposed antenna at both frequencies. The highest current density at 2.4 GHz occurs at the feedline and the inner margins of the radiating structure. This makes sure that the lower ISM band has strong coupling and efficient radiation.

At 5.8 GHz, the current is more spread out along the patch's outer and radiating edges, indicating that higher-order modes

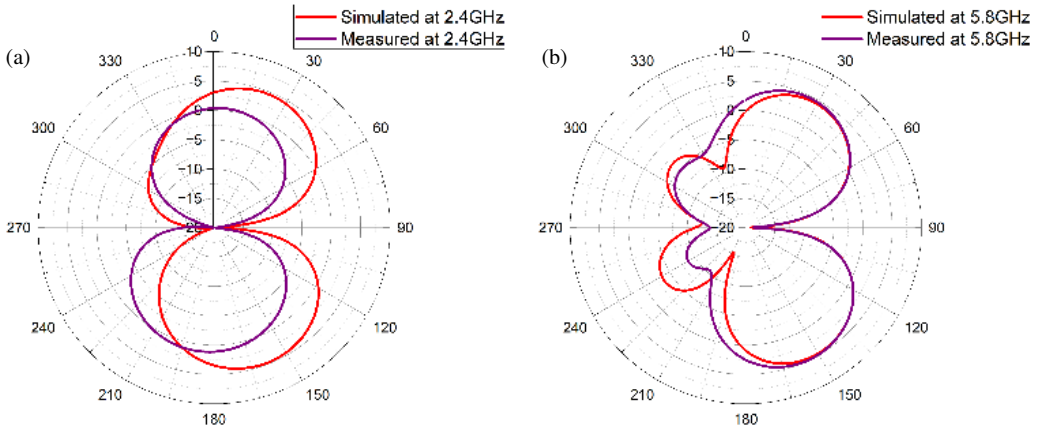

FIGURE 8. Simulated and measured 2D radiation characteristics at (a) 2.4 GHz and (b) 5.8 GHz.

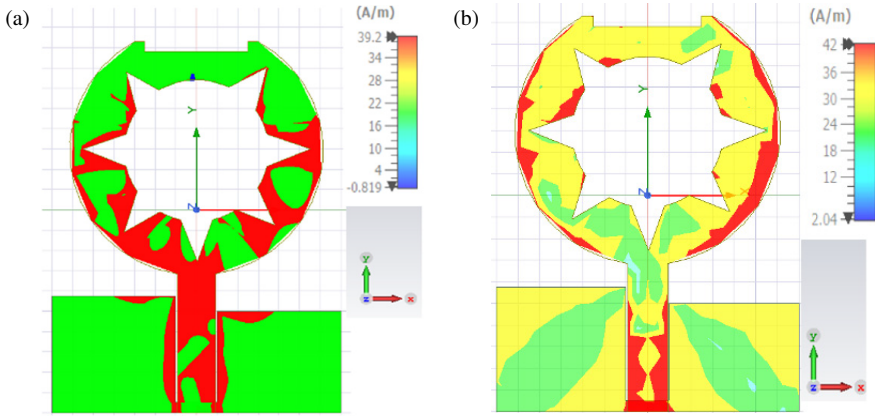

FIGURE 9. The compact IoT-enabled wearable antenna current density at (a) 2.4 GHz, (b) 5.8 GHz.

are excited well for functioning in the upper ISM band. The current patterns we saw show that the antenna works well for dual-band operation.

3.3. On-Body Performance Evaluation

An on-body test was performed to determine the practical performance of the proposed antenna in the presence of body-loading conditions to put the antenna on a human body phantom model, as illustrated in Fig. 10. The simulated on-body S_{11} results indicate that the antenna has an acceptable impedance similar to that near the desired ISM bands at 2.4 GHz and 5.8 GHz, with just a minor resonance shift because of the high permittivity and lossy nature of the human tissues.

The radiation patterns at 2.4 GHz and 5.8 GHz show that the antenna maintains a stable radiation pattern, although there is a slight loss of gain due to the presence of a human phantom model. These findings substantiate the claim that the suggested antenna is stable in practice, even under wearable conditions.

3.4. Specific Absorption Rate (SAR) Evaluation

The SAR evaluation of the wearable antenna was performed using High Frequency Structure Simulator (HFSS) as shown in Fig. 11. The proposed SAR analysis was conducted on a wearable antenna using a human torso phantom model, which represents the practical placement of the antenna for vital signs monitoring. The antenna was placed on the chest region of the phantom with a 2 mm gap, and SAR was calculated for 1 g of tissue at both operating frequencies. The SAR values were 0.6 W/kg at 2.4 GHz and 0.8 W/kg at 5.8 GHz, both of which are significantly lower than the Federal Communications Commission (FCC) safety limit of 1.6 W/kg, indicating that the proposed wearable antenna operates safely.

This makes it a good choice for wearable IoT-based crucial signal transmission applications, in which reliable performance and a small size are important. Table 2 compares the results of this investigation with those of other studies, which proves that the designed antenna is up to the required specifications and is effective.

4. IOT SYSTEM ARCHITECTURE WITH ESP8266 & NODE-RED

To facilitate the secure and dependable wireless transmission of vital signs data wirelessly, the proposed Internet of Things system includes a compact wearable antenna that was custom designed and operated at 2.4 GHz and 5.8 GHz. To prevent interference and guarantee that all transmissions are directed

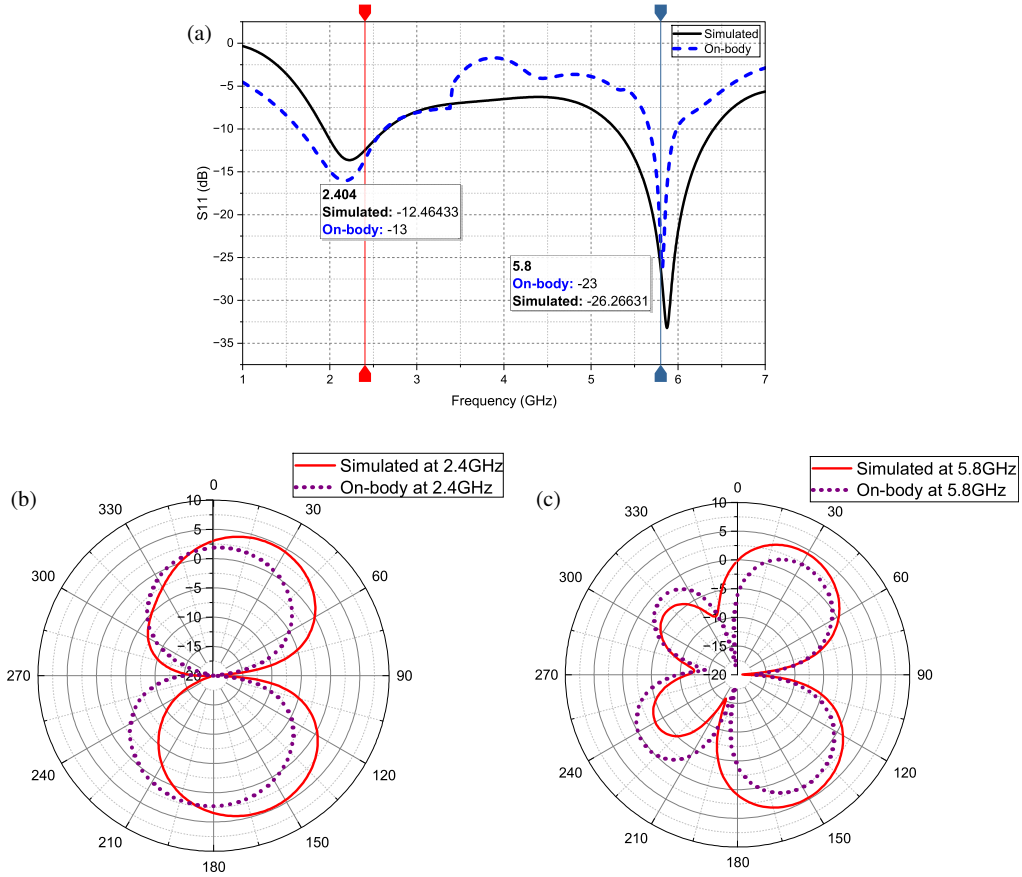

FIGURE 10. On-body performance, (a) S_{11} characteristics, (b) radiation characteristics at 2.4 GHz, and (c) radiation characteristics at 5.8 GHz.

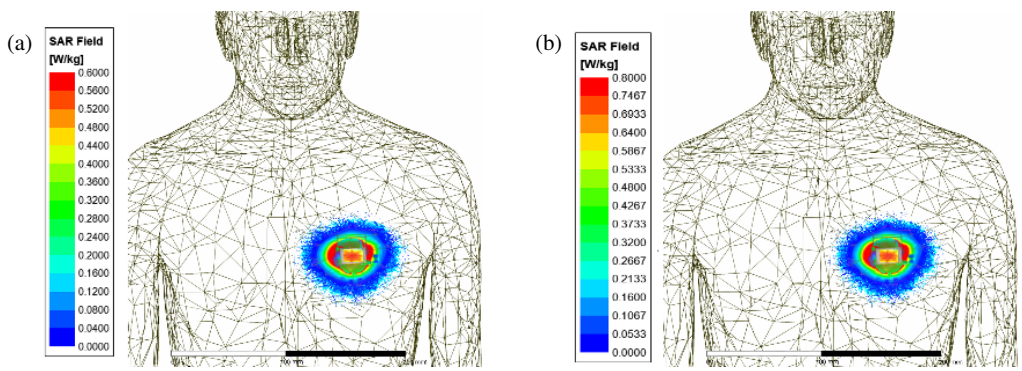

FIGURE 11. The proposed antenna SAR evaluation on human head phantom model, (a) at 2.4 GHz, (b) at 5.8 GHz.

through the fabricated antenna, the internal Wi-Fi antenna of the ESP8266 was intentionally disabled using an RF absorbing material. This dual-band antenna replaced the internal Wi-Fi antenna. Using the Modbus protocol, the ESP8266 acquires physiological signals, including temperature and pulse rate, from connected biomedical sensors and transmits the data over Wi-Fi. Node-RED subscribes to these data streams on the receiver side, processes them, and displays real-time visualizations through a web-based interface. Fig. 12 shows the biomedical sensing system, which is extremely suitable for wearable healthcare monitoring applications owing to the integration of the custom antenna, which improves signal strength, transmission stability, and range.

4.1. Integration of the MAX30100 Biomedical Sensor

The MAX30100 is a low-power, compact optical sensor equipped with two critical biomedical monitoring functions: pulse oximetry and heart-rate measurement, as shown in Fig. 13. It is highly suited for wearable health monitoring applications due to its integration of a red LED, infrared LED, photodetector, and analog signal processing components in a single module. The sensor functions by emitting light into the skin and measuring the variations in light absorption, which are correlated with pulse rate and blood oxygen saturation (SpO_2). The MAX30100 is connected to the ESP8266 microcontroller via the I^2C protocol in the proposed system to facilitate real-time data acquisition. The MAX30100 is an optimal choice

TABLE 2. Comparison of the proposed antenna against the literature.

S.No	Dimensions (mm^3)	Operating Frequency (GHz)	Substrate & Type	Gain (dBi)	Efficiency (%)
[3]	$27 \times 28 \times 0.7$	3.4/7.3/11.8	Denim jeans & Flexible	5.81	90
[5]	$28 \times 21 \times 1.6$	2.4	Rogers 5880 & Semi-flexible	1.95	98
[11]	$59 \times 55 \times 0.1$	2.45	Liquid crystal polymer & Flexible	6.584	75.8
[16]	$45 \times 35 \times 2.5$	2.4	Polydimethylsiloxane & Flexible	6.09	70
[20]	$70.4 \times 76.14 \times 3.11$	1.57/2.45	Rogers & Semi-flexible	5.5	70
Proposed Antenna	$40 \times 28 \times 0.1$	2.4/5.8	Polymide & Flexible	6.45/6.86	85.45/87.55

Note: Gain values of the proposed antenna are measured results, while other values are reported from the respective references.

FIGURE 12. Block diagram of the biomedical sensing system using a wearable antenna.

FIGURE 13. MAX30100.

for continuous monitoring in IoT-based biomedical systems owing to its low power consumption and compact dimensions. Its seamless remote monitoring of vital signs through the Node-RED interface is made possible by its integration with a dual-band antenna and wireless data transmission architecture.

4.2. ESP8266 Setup

ESP8266 microcontroller functions as the primary processing and communication mechanism for the acquisition and transmission of biomedical data. The analog and digital input pins of the ESP8266 are connected to suitable sensors that are used to measure physiological parameters, such as body temperature and pulse rate. Arduino IDE was employed to program the ESP8266 and configure it to function as a Modbus protocol over Wi-Fi. The ESP8266 module only supports 2.4 GHz, so the experiment of data transmission was conducted at this frequency, but the 5.8 GHz resonance suggests that the antenna can support dual-band applications. To guarantee a dedicated and efficient wireless transmission through the fabricated proposed wearable antenna, the ESP8266's onboard printed circuit board (PCB) antenna was disabled using an RF absorbing material, as shown in Fig. 14. The primary data link in the IoT architecture is formed by ESP8266, which publishes sensor data to a Modbus at regular intervals. This configuration guarantees seamless integration with the Node-RED-based monitoring interface and precise data acquisition.

This ensured that all wireless communications only occurred through the proposed wearable antenna. To prevent interference during testing, a foam absorber with carbon was carefully placed over the internal antenna to block its radiation. Using Eccosorb AN-77, which has excellent attenuation properties in the lower ISM band, ensured that the ESP8266 only transmitted signals through the wearable antenna that was linked to the outside. This setup made it possible to accurately test how well the antenna worked in applications that provided vital signs, signal leakage from the internal antenna, and maintaining controlled RF behavior for experimental validation.

4.3. NODE-RED Architecture

Node-RED serves as the IoT visualization and data processing platform in the proposed system data flow diagram shown in Fig. 15. It is configured through the Modbus protocol by the ESP8266, which transmits real-time vital signs data, such as heart rate and temperature. Within the Node-RED flow, Modbus input nodes receive the data, which are then parsed using function nodes and displayed on an interactive web-based dashboard using gauges and charts. This architecture enables real-time monitoring, data logging, and alert generation, offering a user-friendly interface for biomedical signal visualization in remote health monitoring applications. Fig. 16 shows the Node-RED implementation used to obtain and display important biological signals, such as blood oxygen saturation (SpO_2) and heart rate, from the MAX30100 sensor attached to the ESP8266 module. The flow begins with two different timestamp input nodes, one for obtaining data for SpO_2 measurements and the other for obtaining data for heart rate measurements. The timestamp node activates the SpO_2 function block, which processes the sensor data for the SpO_2 path.

The timestamp node also sends data to the heart rate function block for heart rate. This output is sent to a debug node for

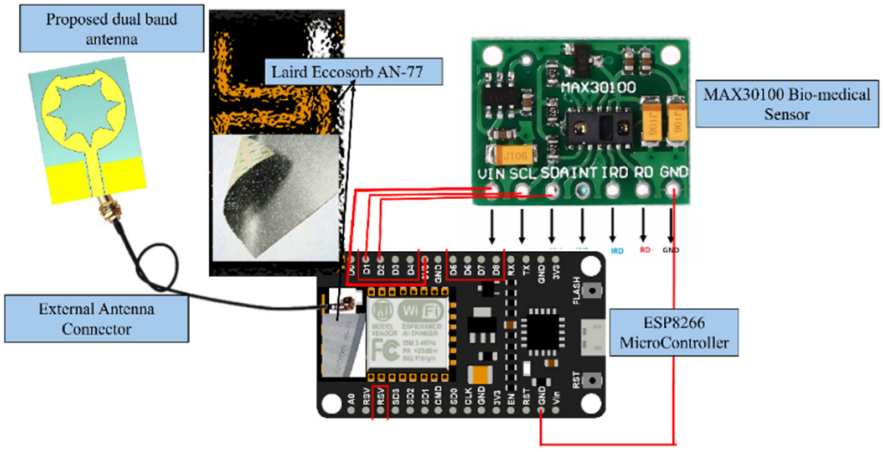

FIGURE 14. Experimental setup of the compact IoT-enabled wearable antenna integrated with the biomedical sensing system.

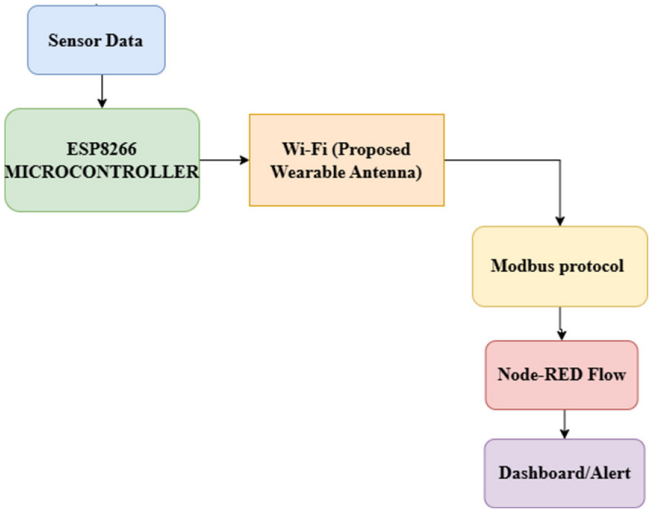

FIGURE 15. Dataflow of node-red architecture.

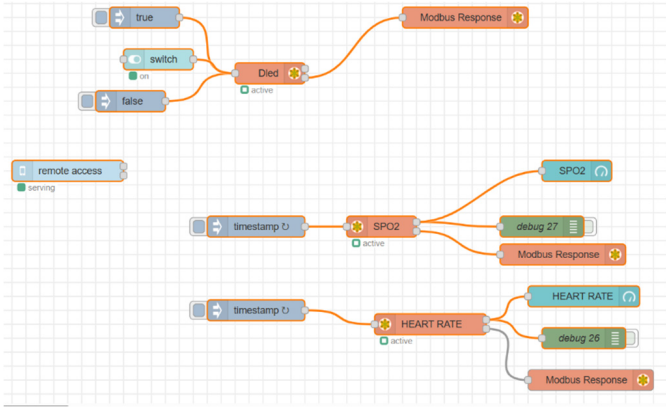

FIGURE 16. Node-RED architecture for SPO_2 and heart rate data acquisition and visualization.

monitoring, a Modbus response node for system interfacing, and a heart rate gauge node for real-time graphical display. This modular flow makes it possible to see, monitor, and maybe even send vital signs data from afar.

4.4. Hardware Integration & Results Evaluation

The hardware integration involved connecting the MAX30100 biomedical sensor to the ESP8266 microcontroller. The built-in Wi-Fi antenna was turned off using Laird Eccosorb AN-77 absorber material and replaced with the proposed dual-band antenna to improve wireless performance, as shown in Fig. 17(a). This arrangement ensured that SpO_2 and heart rate data were collected and transmitted reliably. Node-RED flows were used for real-time monitoring, data debugging, and managing Modbus-based responses. The system was tested by comparing the measured SpO_2 and heart rate values with those of reference medical equipment. Fig. 17(b) shows the experimental validation of the proposed system. It shows how the dual-band wearable antenna was connected to the ESP8266 microprocessor and MAX30100 biomedical sensor. This configuration enabled the acquisition of vital signs in real time.

The Node-RED dashboard showed a heart rate of 84 beats per minute and a SpO_2 level of 97%. Both numbers are within the usual range for the body. A resting heart rate of 60–100 beats per minute and an oxygen saturation level above 95% are both indicators of good health. The ability of the proposed antenna [23] to communicate practically was tested through an experimental transmission experiment by changing the distance between the antenna-integrated ESP8266 module and the mobile hotspot serving as the Wi-Fi access point. The Node-RED cloud dashboard received and displayed biomedical sensor data sent in the Modbus protocol at each distance in real time. The effective data reception proves the high quality of wireless data transmission with the suggested antenna. The communication performance measured at the various distances is presented in Table 3.

These results show that the suggested antenna can reliably send biomedical data wirelessly and make sure that the accuracy is clinically appropriate, which proves that it is good for wearable IoT-based healthcare monitoring applications. To further confirm the efficiency of the proposed antenna-based IoT health monitoring system, vital sign measurements were obtained from people of different ages, as shown in Fig. 17(c). The Node-RED dashboard displayed the heart rate and SpO_2

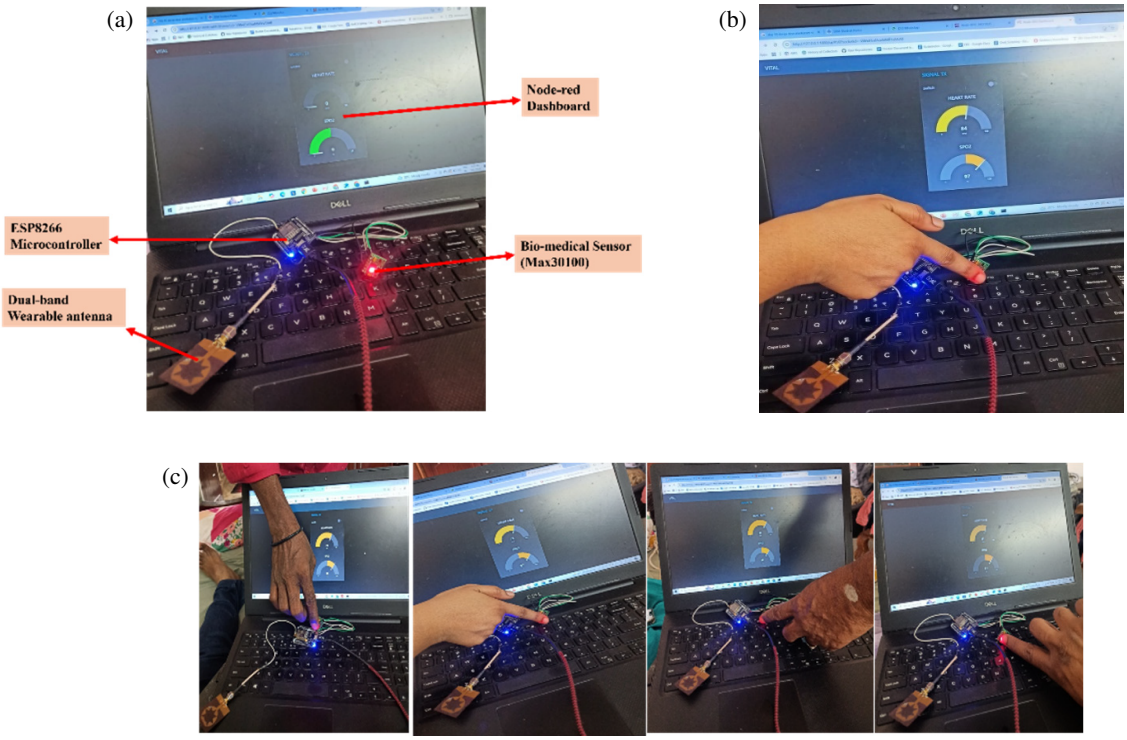

FIGURE 17. (a) Hardware implementation; (b) vital signs data transfer to Node-RED cloud platform; (c) results evaluation on age-grouped people.

TABLE 3. Proposed antenna wireless data transmission performance.

Range	RSSI (dBm)	Data Transmission	Node-RED Dashboard
1 m	−42	Successful	Data Received
3 m	−50	Successful	Data Received
5 m	−58	Successful	Data Received
8 m	−65	Successful	Data Received

*RSSI — Received Signal Strength Indicator

readings for all test subjects, demonstrating that the wireless transmission and sensor performance were reliable. There were minor variations in the measured values owing to age-related physiological variables.

5. CONCLUSION

The article has presented a miniature circular patch antenna for wearable IoT-based healthcare solutions that use 2.4 GHz and 5.8 GHz ISM frequencies. The proposed antenna has a stable dual-band operation with good impedance matching, high radiation efficiency, and reasonable gain characteristics. The SAR analysis establishes that the antenna is functional within the wearable safety limits. The combination of the antenna with an ESP8266-based IoT solution was able to transmit and visualize biomedical data in real time with the help of the Modbus protocol and Node-RED dashboard. The experimental findings indicate that the proposed antenna is a good and reliable miniature solution to wearable wireless healthcare monitoring systems.

REFERENCES

[1] Rodrigues, J. J. P. C., D. B. De Rezende Segundo, H. A. Junqueira, M. H. Sabino, R. M. Prince, J. Al-Muhtadi, and V. H. C. De Albuquerque, "Enabling technologies for the internet of health things," *IEEE Access*, Vol. 6, 13 129–13 141, 2018.

[2] Boca, L. L., E. M. Ciortea, C. Boghean, A. Begov-Ungur, F. Boghean, and V. T. Dădârlat, "An IoT system proposed for higher education: Approaches and challenges in economics, computational linguistics, and engineering," *Sensors*, Vol. 23, No. 14, 6272, 2023.

[3] Maria, A. and P. Mythili, "Compact UWB wearable textile antenna for on-body WBAN applications," *Progress In Electromagnetics Research B*, Vol. 105, 43–57, 2024.

[4] Zhang, Q., D. Soham, Z. Liang, and J. Wan, "Advances in wearable energy storage and harvesting systems," *Med-X*, Vol. 3, No. 1, 3, 2025.

[5] Zambak, M. F., S. S. Al-Bawri, M. Jusoh, A. H. Rambe, H. Vettikalladi, A. M. Albishi, and M. Himdi, "A compact 2.4 GHz L-shaped microstrip patch antenna for ISM-band Internet of Things (IoT) applications," *Electronics*, Vol. 12, No. 9, 2149, 2023.

[6] Thanh, T. N., M. C. Nguyen, M. T. Le, N. Q. Dinh, Q. C. Nguyen, K. Nguyen, and H. Le-Minh, "A novel energy-efficient health monitoring system with electromagnetic-reducing dual-band antenna," *IEEE Sensors Journal*, Vol. 25, No. 10, 18 201–18 212, 2025.

[7] De-La-Fuente-Robles, Y.-M., A.-J. Ricoy-Cano, A.-P. Albín-Rodríguez, J. L. López-Ruiz, and M. Espinilla-Estévez, "Past, present and future of research on wearable technologies for healthcare: A bibliometric analysis using scopus," *Sensors*, Vol. 22, No. 22, 8599, 2022.

[8] Al-Sehemi, A., A. Al-Ghamdi, N. Dishovsky, N. Atanasov, and G. Atanasova, "Design and performance analysis of dual-band wearable compact low-profile antenna for body-centric wire-

less communications," *International Journal of Microwave and Wireless Technologies*, Vol. 10, No. 10, 1175–1185, 2018.

[9] Abbasi, M. A. B., S. S. Nikolaou, M. A. Antoniades, M. N. Stevanović, and P. Vryonides, "Compact EBG-backed planar monopole for BAN wearable applications," *IEEE Transactions on Antennas and Propagation*, Vol. 65, No. 2, 453–463, 2017.

[10] Madjar, H. M., "Human radio frequency exposure limits: An update of reference levels in Europe, USA, Canada, China, Japan and Korea," in *2016 International Symposium on Electromagnetic Compatibility — EMC EUROPE*, 467–473, Wroclaw, Poland, 2016.

[11] El Atrash, M., O. F. Abdalgalil, I. S. Mahmoud, M. A. Abdalla, and S. R. Zahran, "Wearable high gain low SAR antenna loaded with backed all-textile EBG for WBAN applications," *IET Microwaves, Antennas & Propagation*, Vol. 14, No. 8, 791–799, 2020.

[12] Das, G. K., S. Basu, B. Mandal, D. Mitra, R. Augustine, and M. Mitra, "Gain-enhancement technique for wearable patch antenna using grounded metamaterial," *IET Microwaves, Antennas & Propagation*, Vol. 14, No. 15, 2045–2052, 2020.

[13] Yan, S., P. J. Soh, and G. A. E. Vandenbosch, "Low-profile dual-band textile antenna with artificial magnetic conductor plane," *IEEE Transactions on Antennas and Propagation*, Vol. 62, No. 12, 6487–6490, 2014.

[14] Karad, K. V. and V. S. Hendre, "A foam-based compact flexible wideband antenna for healthcare applications," *Progress In Electromagnetics Research C*, Vol. 123, 197–212, 2022.

[15] Atanasova, G. and N. Atanasov, "Small antennas for wearable sensor networks: Impact of the electromagnetic properties of the textiles on antenna performance," *Sensors*, Vol. 20, No. 18, 5157, 2020.

[16] Gao, G., S. Wang, R. Zhang, C. Yang, and B. Hu, "Flexible EBG-backed PIFA based on conductive textile and PDMS for wearable applications," *Microwave and Optical Technology Letters*, Vol. 62, No. 4, 1733–1741, 2020.

[17] Karad, K. V., V. S. Hendre, J. L. Rajput, V. Kadam, V. E. Narawade, R. Bakale, and G. D. Londhe, "A SAR analysis of hexagonal-shaped UWB antenna for healthcare applications," *EURASIP Journal on Wireless Communications and Networking*, Vol. 2024, No. 1, 72, 2024.

[18] Varkiani, S. M. H. and M. Afsahi, "Compact and ultra-wideband CPW-fed square slot antenna for wearable applications," *AEU — International Journal of Electronics and Communications*, Vol. 106, 108–115, 2019.

[19] Arif, A., M. Zubair, M. Ali, M. U. Khan, and M. Q. Mehmood, "A compact, low-profile fractal antenna for wearable on-body WBAN applications," *IEEE Antennas and Wireless Propagation Letters*, Vol. 18, No. 5, 981–985, 2019.

[20] Paracha, K. N., S. K. A. Rahim, P. J. Soh, M. R. Kamarudin, K.-G. Tan, Y. C. Lo, and M. T. Islam, "A low profile, dual-band, dual polarized antenna for indoor/outdoor wearable application," *IEEE Access*, Vol. 7, 33 277–33 288, 2019.

[21] Wagih, M., Y. Wei, and S. Beeby, "Flexible 2.4 GHz node for body area networks with a compact high-gain planar antenna," *IEEE Antennas and Wireless Propagation Letters*, Vol. 18, No. 1, 49–53, 2019.

[22] Rattanapoka, C., S. Chanthakit, A. Chimchai, and A. Sookkeaw, "An MQTT-based IoT cloud platform with flow design by Node-RED," in *2019 Research, Invention, and Innovation Congress (RI2C)*, 1–6, Bangkok, Thailand, 2019.

[23] Karad, K. V. and V. S. Hendre, "A hexagonal shape fractal flexible UWB antenna based on jeans material for healthcare applications," *The Journal of the Textile Institute*, Vol. 116, No. 7, 1227–1242, 2025.